Ann. Geophys., 25, 207–218, 2007
www.ann-geophys.net/25/207/2007/

Annales Geophysicae

Earth conductivity structures and their effects on geomagnetic induction in pipelines

P. A. Fernberg[1,2], **C. Samson**[1], **D. H. Boteler**[2], **L. Trichtchenko**[2], **and P. Larocca**[3]

[1]Dept. of Earth Sciences, Carleton University, 1125 Colonel By Drive, Ottawa, ON, K1S 5B6, Canada
[2]Natural Resources Canada, 7 Observatory Crescent, Ottawa, ON, K1A 0Y3, Canada
[3]Engineering School, University of Buenos Aires, Paseo Colón 750 Buenos Aires, Argentina

Received: 11 September 2006 – Revised: 8 January 2007 – Accepted: 11 January 2007 – Published: 1 February 2007

Abstract. Anomalous, large pipe-to-soil potentials (PSP) have been observed along a natural gas pipeline in eastern Ontario, Canada, where there is a major geological contact between the highly resistive rocks of the Precambrian Shield to the west and the more conductive Paleozoic sediments to the east. This study tested the hypothesis that large variations of PSP are related to lateral changes of Earth conductivity under the pipeline. Concurrent and co-located PSP and magnetotelluric (MT) geophysical data were acquired in the study area. Results from the MT survey were used to model PSP variations based on distributed-source transmission line theory, using a spatially-variant surface geoelectric field. Different models were built to investigate the impact of different subsurface features. Good agreement between modelled and observed PSP was reached when impedance peaks related to major changes of subsurface geological conditions were included. The large PSP could therefore be attributed to the presence of resistive intrusive bodies in the upper crust and/or boundaries between tectonic terranes. This study demonstrated that combined PSP-MT investigations are a useful tool in the identification of potential hazards caused by geomagnetically induced currents in pipelines.

Keywords. Geomagnetism and paleomagnetism (Geomagnetic induction; Instruments and techniques; General or miscellaneous)

1 Introduction

Fluctuating electrical currents flowing in the ionosphere and magnetosphere resulting from solar disturbances (flares, coronal mass ejections) create variations of the Earth's magnetic field. These geomagnetic variations induce a geoelectric field at the Earth's surface and interior. The geoelectric field in turn drives geomagnetically induced currents (GIC) – also called telluric currents – along electrically conductive technological networks, such as power transmission lines, railways and pipelines (Lanzerotti and Gregori, 1986), and may cause serious harm to the infrastructure.

GIC in pipelines interfere with cathodic protection systems, disrupt pipeline surveys, and create conditions where enhanced corrosion may occur (Gummow, 2002). It is common practice to make pipeline surveys once a year to measure the voltage at test posts to ensure that pipe-to-soil potential (PSP) variations are within the safe range (-850 to -1150 mV) impressed by cathodic protection systems. The PSP readings, however, are often irregular and at times fall outside the recommended range. Their interpretation is difficult because several factors can influence PSP measured locally at a given time:

- The geomagnetic activity (both the magnitude and frequency of magnetic variations);
- The Earth conductivity profile beneath the pipeline; and,
- The pipeline structure (the presence of bends, flanges and terminations, the splitting or merging of one or two pipes, coating) and orientation.

The influence of geomagnetic activity on PSP has been studied in many places, e.g. Campbell (1978, 1980), Boteler et al. (1998), Pulkkinen et al. (2001a, b), and Hejda and Bochníček (2005). Earth conductivity contrasts can create amplitude variations of surface geoelectric fields resulting in noticeable GIC variations (Osella and Favetto, 2000), in particular where a pipeline crosses a highly resistive intrusive rock. Geoelectric field amplitude and phase can undergo a complex redistribution due to crustal-scale variations of resistivity, particularly at boundaries of tectonic terranes (Beamish et al., 2002). Variations of the geoelectric field in northern England were attributed to complex crustal structure, area faulting and conductive anomalies (McKay and

Correspondence to: P. A. Fernberg
(pfernbe2@connect.carleton.ca)

Published by Copernicus GmbH on behalf of the European Geosciences Union.

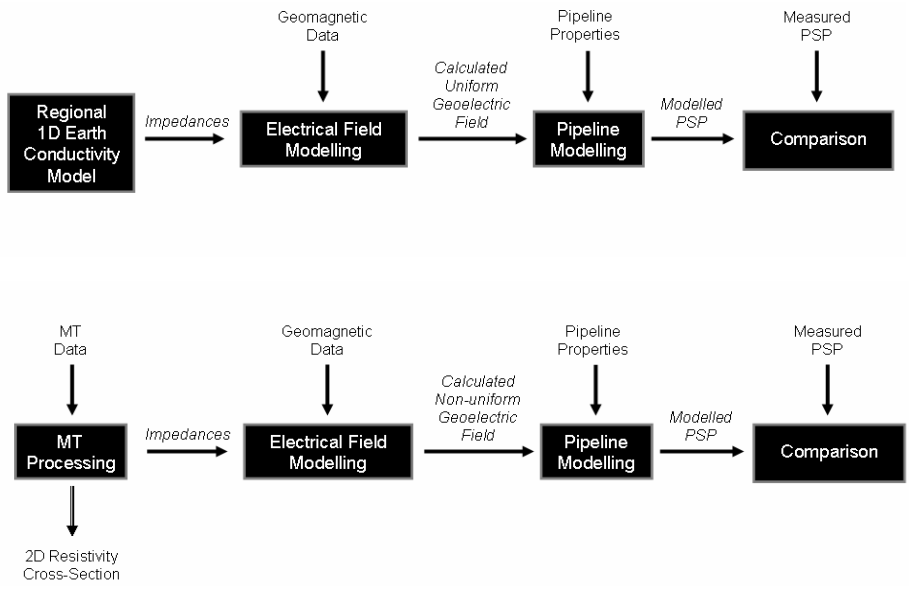

Fig. 1. Two schemes of PSP modelling. The bottom scheme takes into account the non-uniform (2-dimensional) geological conductivity variations along the pipeline route.

Whaler, 2006). Changes in pipeline structure and orientation and their effects on PSP are discussed in Boteler (2000), Boteler and Trichtchenko (2000), Gummow et al. (2001), and Rix and Boteler (2001).

This paper focuses on the relation between Earth conductivity structures and PSP fluctuations (Fig. 1). The first step in understanding this relation quantitatively is to calculate the surface geoelectric field, which drives the GIC in pipelines. The surface geoelectric field is easily calculated from the surface magnetic field (i.e. obtained from magnetic observatory data) by combining it with the surface impedance derived from a regional one-dimensional (1-D) Earth conductivity model. The 1-D model assumes that the Earth conductivity varies only with depth and ignores lateral conductivity variations (Fig. 1, top). Initial PSP modelling studies have assumed uniform geomagnetic and geoelectric fields over the pipeline route, as well as a uniform or layered Earth (Pulkkinen et al., 2001b; Trichtchenko and Boteler, 2002; Hejda and Bochníček, 2005).

The uniform electromagnetic field approximation may be valid only in specific areas during limited time periods. Therefore, non-uniform geoelectric fields are likely to be the norm due to a real Earth conductivity being neither uniform nor layered (Pirjola, 2002), and that sources of geomagnetic field variations (the ionosphere currents) have finite dimension and duration. Different methods of calculating the uniform and non-uniform surface geoelectric and magnetic fields produced by structural external (ionosphere) sources can be found in Pirjola (2002) and references therein).

In our study we consider a non-uniform geoelectric field caused by internal sources, i.e. non-uniform Earth conductivities. Surface impedances are calculated from magnetotelluric (MT) measurements at multiple sites along a profile parallel to the pipeline route. These are used to calculate a non-uniform surface geoelectric field (Fig. 1, bottom). This more representative approach shows the response of the geoelectric field to lateral variations in geological conductivity, therefore taking into account the 2-D Earth conductivity structure beneath the pipeline.

The pipeline investigated is part of a transcontinental natural gas pipeline that extends 3100 km from the Alberta/Saskatchewan border east to Quebec/Vermont, connecting with other pipelines in Canada and the U.S. In 1997, Boteler and Trichtchenko (2000) undertook a detailed study along a 450 km long branch of this pipeline in eastern Ontario, measuring PSP from eleven sites evenly distributed along the pipeline route. Possible changes in the pipeline structure and orientation alone could not explain the large differences in PSP amplitude between the different sites surveyed in the 1997 study. Boteler et al. (2003) proposed that an additional effect might be lateral changes in Earth conductivity because the largest PSP variations were recorded in the proximity of a major geological contact between the highly resistive rocks ($\approx$10 000 Ω m) of the Canadian Precambrian Shield to the west and the less resistive ($\approx$10 Ω m) Paleozoic sediments to the east (Telford et al., 1976). The main objective of our investigation was to test that hypothesis. Secondary objectives were to identify more precisely the zone along the pipeline where large PSPs are observed and to investigate what geological structures can cause significant electrical conductivity contrasts in the study area.

Table 1. Survey statistics and instrument specifications.

		PSP		MT	
Survey		2003 ORV	2005 ORF	2003 ORV	2005 ORF
Number of Sites		9	39	4	17
Site Spacing		9 km	3 km	25 km	6 - 9 km
Instrumentation	Manufacturer	Cath-Tech	Tinker-Rasor	Phoenix Geophysics	
	Instrument	HEXCORDER Millennium DataLogger	DL - 1 Data Logger	MTU-5A Central Processing Unit	
	Sampling Frequency	1 Hz	5 Hz	15 Hz	
	Number of Channels	1	1	5 (electric: Ex, Ey) (magnetic: Hx, Hy, Hz)	
	Timing Reference	GPS	Internal Clock	GPS	
	Data Storage Capacity	1 Mb	500,000 samples	128 - 512 kb	
	Power Source	Internal Battery	Internal Battery	External Battery	

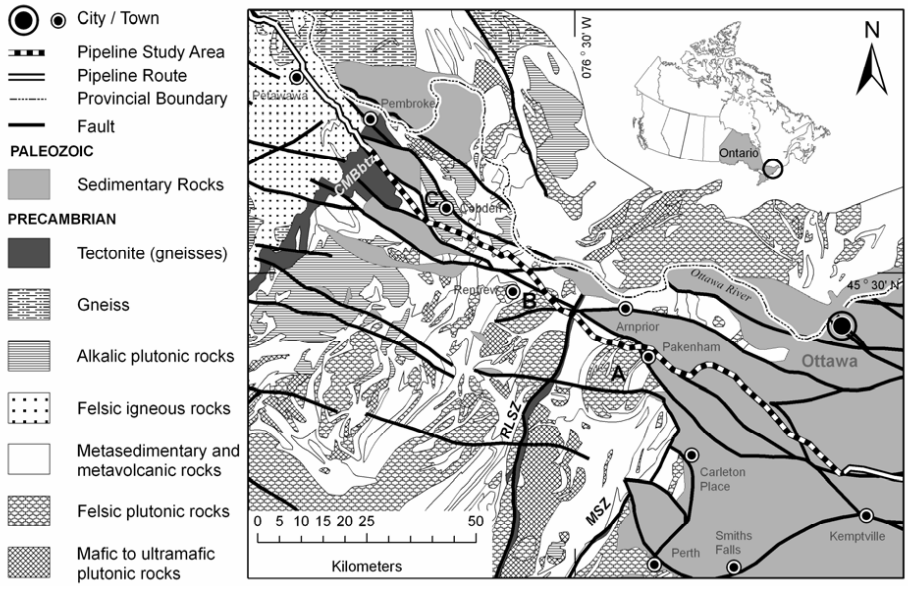

Fig. 2. Bedrock geology map of the Ottawa River valley and region, crossed by the pipeline. Tectonic units: CMBbtz, Central Metasedimentary Belt boundary thrust zone; RLSZ, Robertson Lake Shear Zone; MSZ, Maberly Shear Zone. Intrusives: A, Pakenham Dome; B, Hurds Lake; C, Bonnechere Ridge (modified from Ontario Geological Survey, 1993).

2 Surveys

In support of the above objectives, two combined PSP and MT surveys (Table 1) were conducted along a 155 km long section of the pipeline in the Ottawa River Valley: the 2003 ORV (4 October 2003–10 October 2003) (Trichtchenko et al., 2004) and 2005 ORF (31 May 2005–11 June 2005) surveys. This area was selected because it brackets the zone of high PSP variations previously identified in the 1997 study and features the two major tectonic units of contrasting resistivity: the Precambrian Grenville Province to the west and the Paleozoic Ottawa Embayment to the east (Fig. 2).

The Grenville Province is a complex blend of highly deformed and metamorphosed rocks (granite, gneiss, marble, quartzite) representing several cycles of continental-scale collision and subduction 1500 to 900 million years ago (Carr et al., 2000). The result is a crustal architecture consisting of accreted tectonic terranes separated by northeasterly trending shear zones, many of which penetrate the full thickness of the crust (Percival et al., 2004). Intrusive bodies of late to middle Precambrian age are numerous. Paleozoic sedimentary rocks of the Ottawa Embayment (Sanford, 1993) cover the eastern half of the Grenville basement rocks in the study area, and also occur as inliers in the western half. Flat-lying Ordovician sandstone, shale, dolostone and limestone can be up to 150 m thick, shallowing to the west. Unconsolidated sediments in the Ottawa Valley study area consist of glacial tills, and paleo-Champlain Sea marine clays and silts locally known as Leda clay (Belanger, 1998).

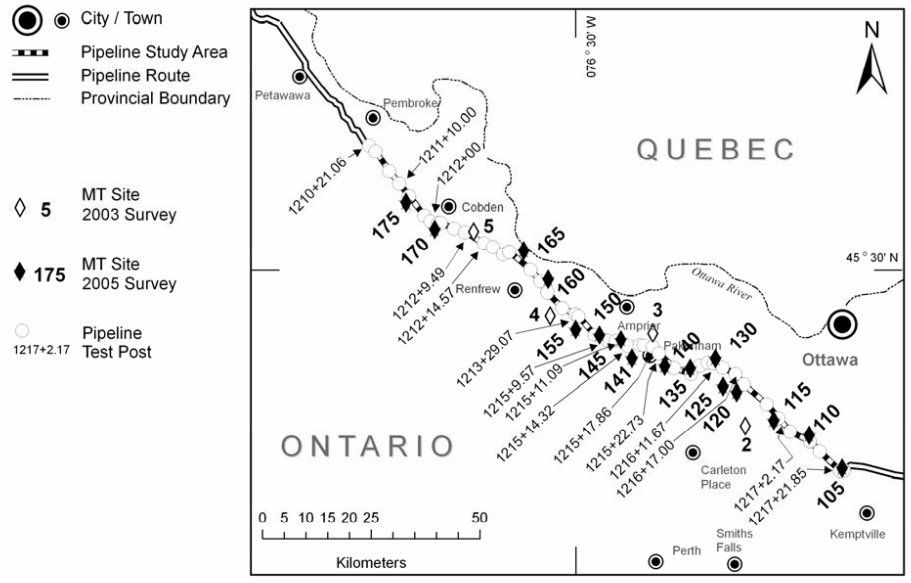

Fig. 3. Location of individual MT sites and test posts along the study area. Test posts near a MT site are marked with identification numbers.

Within the study area, the pipeline crosses Paleozoic sedimentary rock, Precambrian metasediments (marble dominant) and metavolcanics, intrusives and a band of tectonite. Felsic plutonic rock forms two of the larger intrusives (the Pakenham Dome granite and granodiorite and the Hurds Lake trondhjemite) beneath the pipeline route. An alkalic plutonic rock (the Bonnechere Ridge syenite) forms the third large intrusive along the pipeline corridor. From southeast to northwest the pipeline crosses four Grenvillian tectonic terranes: Frontenac, Sharbot Lake, Mazinaw, and the Bancroft. Major, north-easterly trending, shear zones cross the pipeline route and form boundaries between the different terranes. These include the Robertson Lake Shear Zone and the Maberly Shear Zone, the latter may cross the pipeline route beneath the covering Paleozoic sediments. Part of the pipeline route follows the north-westerly trending Pakenham Fault which forms a partial boundary between the Precambrian and Paleozoic rocks.

Electrical resistivity contrasts of crustal rocks in the study area would likely be significant due to the geological variability in south-eastern Ontario. Generally, intrusives have the highest resistivity, metamorphic rocks are intermediate, and consolidated sediments the lowest, depending on local porosity, salinity of contained water and lithological conditions (Telford et al., 1976). Depending on the salinity of the local Leda clay its electrical resistivity can vary widely, ranging from 1–20 Ω m (J. Hunter, personal communication, 2006).

During the MT surveys, the two horizontal components of the surface geoelectric field, E_x and E_y, were recorded by electrodes at the ends of 100 m long wire dipoles oriented magnetic north-south and east-west, respectively. The three components of the geomagnetic field, H_x, H_y and H_z, were recorded by induction coils oriented magnetically north-south, east-west and vertically, respectively. The MT surveys covered a frequency range between 0.001 to 10 000 Hz. Geomagnetic variations between 10–10 000 Hz, recorded by audio-magnetotelluric (AMT) coils, penetrate the top portion of the crust, to a depth of 5 to 10 km (Jones and Garcia, 2006). The longer period variations from 0.001–400 Hz, recorded by broad-band MT coils, penetrate down to upper mantle depths of about 600 km (Simpson and Bahr, 2005). Data were time referenced using the global positioning system. MT sites were carefully selected to be at least, where possible, 1.0 km away from the pipeline to minimize electromagnetic interference from the pipeline's cathodic protection system (Fig. 3).

PSP data were acquired by placing small portable data loggers at pre-existing test posts (Fig. 3) along the pipeline. PSP variation is measured, at a 5 Hz sampling frequency, using a high impedance voltmeter electrically connected to a pipe test lead and a reference $Cu/CuS0_4$ electrode placed in the surrounding soil (Bianchetti, 2001). In the study area, test posts were located at least every kilometre along the pipeline and are identified by the distance from a particular valve station. For example, test post 1215+17.86 is located 17.86 km east of valve station 1215.

Figure 4 shows an example of the field data recorded on 8 October 2003. A geomagnetic disturbance occurred between 22:55 and 23:10 universal time (UT). The MT E_x, E_y, H_x and H_y time series from site ORV2, and PSP recordings from test posts 1215+2.84 and 1215+17.86 are plotted together to highlight the coincidence of the variations in the two data sets.

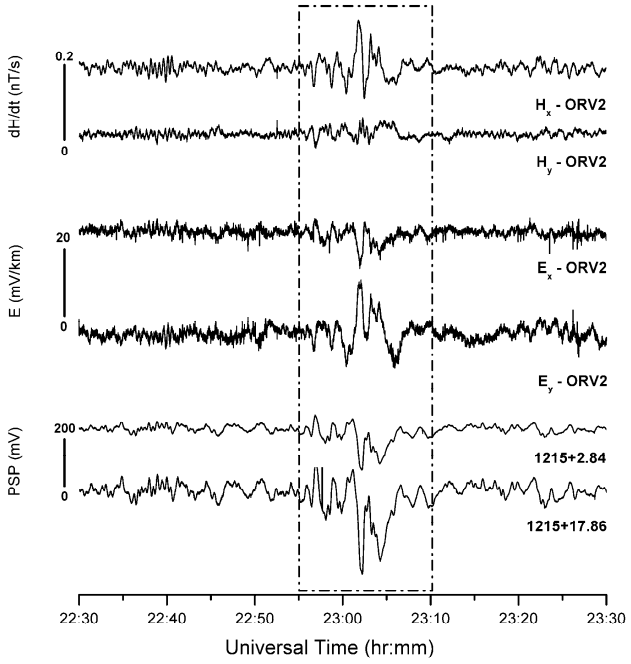

Fig. 4. Field data recorded on 8 October 2003: magnetically oriented north-south (E_x) and east-west (E_y) components of the surface geoelectric field from MT site ORV2; magnetically oriented north-south (dH_x/dt) and east-west (dH_y/dt) components of the geomagnetic field from MT site ORV2; PSP recordings from test posts 1215+2.84 and 1215+17.86. The boxed area emphasizes a geomagnetic disturbance. Geoelectric field data was decimated and plotted at 1 Hz.

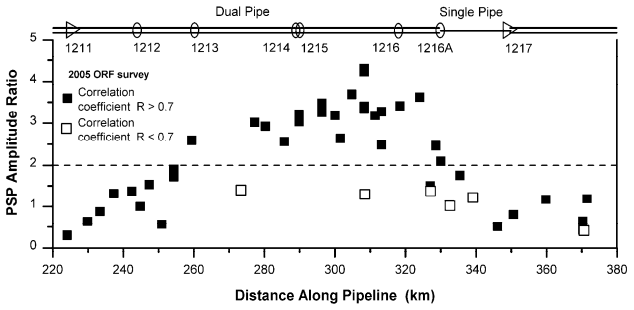

Fig. 5. PSP amplitude ratios (squares) as a function of the distance along pipeline and schematic representation of the pipeline structure (oval represents a main line valve; triangle represents a compressor station). Ratios above the dashed line are considered anomalously large (ratio >2). Distance along pipeline is measured from kilometer point 0 in North Bay.

3 Data analysis

3.1 PSP variations

Visual inspection of the PSP recordings show simultaneous variations at all test posts on any particular survey day. The largest amplitudes were recorded at test post 1215+17.86, within half a kilometre of where the largest amplitudes were observed in 1997 (Boteler and Trichtchenko, 2000).

A comparison of the relative size of PSP variations was done to determine if there was a lateral PSP variability along the pipeline route and whether it correlated with any geological or pipeline features. For each recording day where simultaneous time series measurements were available the data from different test posts were plotted against a reference test post. Scatter plots were prepared to show the PSP time series variation between a particular test post and a reference test post, with the slope of its linear fit giving the PSP amplitude ratio between these two test posts. Forty-five different test post comparisons were made, using the entire PSP time series data for each comparison. Correlation coefficients between PSP time series data were generally greater than 0.8, with only 14% below a value of 0.7.

Test post 1212+00 was chosen as the primary reference because it was operating the longest during the survey and provided good quality data. For those days when no data logger was operating at the primary reference test post (1212+00), secondary reference test posts were used. PSP amplitude ratios computed using the secondary reference test post(s) were referenced back to the primary reference test post in order to obtain the equivalent amplitude ratio with respect to the primary reference.

The PSP amplitude ratios, as a function of the distance along the pipeline (Fig. 5), demonstrate the presence of an anomalous zone of large amplitudes (ratio >2) extending from valve stations 1213 (km 260) to 1216A (km 328). Peak amplitude ratios have been recorded at test post 1215+17.86 (km 308) and drop off in both directions away from this location. The drop off is steeper to the southeast of test post 1215+17.86 where the pipeline structure changes from dual to single to dual pipe. The points which show deviations from the general pattern (open squares in Fig. 5) also have very low correlation (R<0.7) with the reference test post. We compared correlation coefficients against distance between test post locations and found that low coefficients were not necessarily related to large separation between test posts. Low correlations are more likely due to local interference at particular locations, such as loose or broken test post wires, ground conditions preventing good contact for the reference electrode, and nearby presence of rectifiers (cathodic protection system) or other electrical objects like power lines and cattle fences. Therefore, these irregular amplitude ratios can be treated as insignificant.

3.2 MT analysis

Fourteen MT sites (four from the 2003 ORV and 10 from the 2005 ORF surveys) acquired good quality data and were included in the analysis. Unsuitable sites included those contaminated by locally high levels of electrical interference

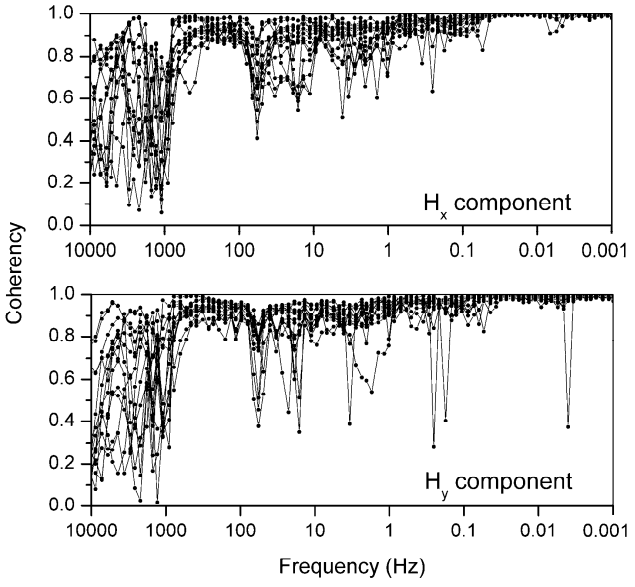

Fig. 6. Coherency between the 14 individual MT sites and their reference sites as a function of frequency for the horizontal geomagnetic components H_x (top) and H_y (bottom).

(electric fencing, dewatering pumps, powerline proximity, railroad traffic) or by instrument failure.

The first step in processing consisted of transforming the MT time series data to the Fourier domain. The remote referencing (Gamble et al., 1979) procedure was applied to data from each of the MT sites to reduce the effects of local noise. The remote referencing method assumes a uniform geomagnetic field over the study area. To check the validity of this assumption the coherency between the geomagnetic signals from individual MT sites and their reference site was computed (Kay, 1993). Figure 6 shows the results of the coherency analysis for the horizontal geomagnetic components H_x and H_y. The overall coherency is above 0.8 for a broad range of frequencies from 0.001 to 1000 Hz. A local coherency minimum at 60 Hz is due to power line noise. Above 1000 Hz, coherency is low because of the weakness of the natural geomagnetic field.

The horizontal and vertical components of the geomagnetic field were used in the computation of induction arrows which are vectorial representations of lateral conductivity variations. Induction arrows for a frequency of 0.01 Hz were found to be perpendicular to the northeast–southwest Grenville structural trend, in agreement with the findings of Frederiksen et al. (2005). The induction arrows also indicated that conductivity is highest at the southeast end of the profile, an observation consistent with the fact that the Paleozoic rocks are overall more conductive than Precambrian rocks in the study area.

After examination of the induction arrows, the measured MT impedances were rotated 45° clockwise so they could be decomposed in components parallel and perpendicular to the regional geoelectric strike. These components can be used to give the transverse magnetic (TM) and transverse electric (TE) impedances. We used the TM impedance for further analysis as it relates the electric field parallel to the pipeline to the magnetic field variations.

Rotated impedances from the 14 MT sites were inverted globally to produce the 2-D resistivity versus depth cross-section presented in Fig. 7. Three, surface exposed, intrusive bodies along the pipeline route approximately coincide with orbicular zones of higher resistivity (1100–5500 Ω m), extending to depths of 6 to 12 km. The Bonnechere Ridge intrusive (C on Fig. 7) has the greatest lateral and vertical extent. The Hurds Lake intrusive (B on Fig. 7) shows up as a moderately sized and defined resistive body. However, the larger Pakenham Dome intrusive (A on Fig. 7) is not as clearly defined in terms of resistivity, perhaps being masked by the covering Paleozoic rock and Leda clay. Two additional orbicular high resistivity bodies situated at the southeast end of the cross-section could be intrusives for they are aligned with exposed intrusives situated just south of the Paleozoic cover rock. Faults generally coincide with zones of lower resistivity between the intrusive bodies. A thin zone of low resistivity (30–80 Ω m) occurs between MT sites ORF140 and ORF145 where conductive Leda clays thicken in the local Mississippi River valley. On the scale of tectonic terranes and at mid to lower crustal depths a large zone of low resistance (45–65 Ω m) is present in the area underlain by the Frontenac terrane. A transitional moderately resistive region (80–225 Ω m) occurs in the area of the Sharbot Lake terrane. A more resistive region (225–800 Ω m) occupies the Mazinaw and Bancroft terranes.

3.3 Geoelectric field

The relation between the horizontal geoelectric and geomagnetic fields can be written in terms of the impedance tensor $\mathbf{Z}$ where the components of the 2×2 matrix are complex ratios of the Fourier coefficients of the horizontal geoelectric and geomagnetic fields, expressed as:

$$\begin{pmatrix} E_x \\ E_y \end{pmatrix} = \begin{pmatrix} Z_{xx} & Z_{xy} \\ Z_{yx} & Z_{yy} \end{pmatrix} \begin{pmatrix} H_x \\ H_y \end{pmatrix}. \quad (1)$$

Because the calculated 2-D geoelectric field is obtained from MT impedances measured in a magnetic-north coordinate system, it was necessary to rotate the measured impedance by 45° clockwise in order to obtain the electric field along the pipeline route. General formulas for rotation of impedance are given by Kaufman and Keller (1981). For the case when θ=45°, cos 2θ=0 and sin 2θ=1, the formulas simplify to:

$$Z_{yx}(45) = 0.5\left[-Z_{xx} - Z_{xy} + Z_{yx} + Z_{yy}\right]. \quad (2)$$

$$Z_{yy}(45) = 0.5\left[Z_{xx} - Z_{xy} - Z_{yx} + Z_{yy}\right]. \quad (3)$$

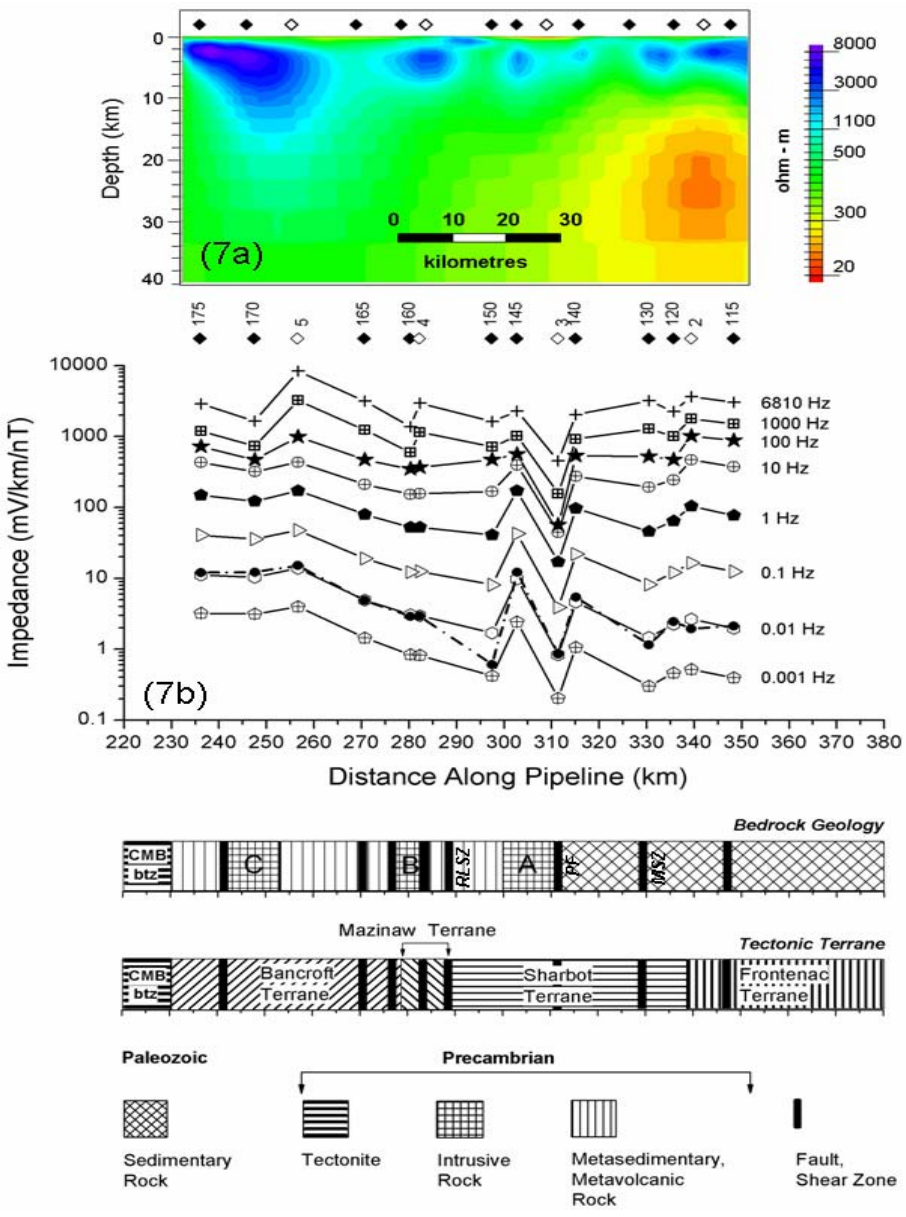

Fig. 7. (a) Resistivity cross-section (TM component) beneath pipeline. **(b)** Measured Z_{yx} (45) surface impedance (dashed line) at 0.01 Hz used as input to pipeline modelling and modelled response Z_{yx} impedance (solid lines) – at eight different frequencies – obtained from resistivity cross-section. MT sites from 2003 ORV (◇) and 2005 ORF (◆) surveys, and schematics of exposed bedrock and tectonic terranes along the pipeline route in study area are shown. Abbreviations: A, Pakenham Dome; B, Hurds Lake; C, Bonnechere Ridge; CMBbtz, Central Metasedimentary Belt boundary thrust zone; RLSZ, Robertson Lake Shear Zone; PF, Pakenham Fault; MSZ, Maberly Shear Zone (possible north-eastward extension).

The geoelectric field along the pipeline can be computed from Eq. (1) using:

$$E_{//} = Z_{yx}(45)H_{\perp} + Z_{yy}(45)H_{//} \quad (4)$$

where // and ⊥ denote parallel and perpendicular to the pipeline route.

Examination of the impedances revealed that Z_{yy} (45) is smaller than Z_{yx} (45) and also has more phase variability. Therefore, the Z_{yy} (45) impedance is not expected to have much influence on the geoelectric field along the pipeline and in order to simplify the analysis, Eq. (4) has been reduced to:

$$E_{//} = Z_{yx}(45)H_{\perp}. \quad (5)$$

Coherency analysis (Fig. 6) has shown that the geomagnetic field variations can be considered uniform over the study area. Therefore the common magnetic field variation

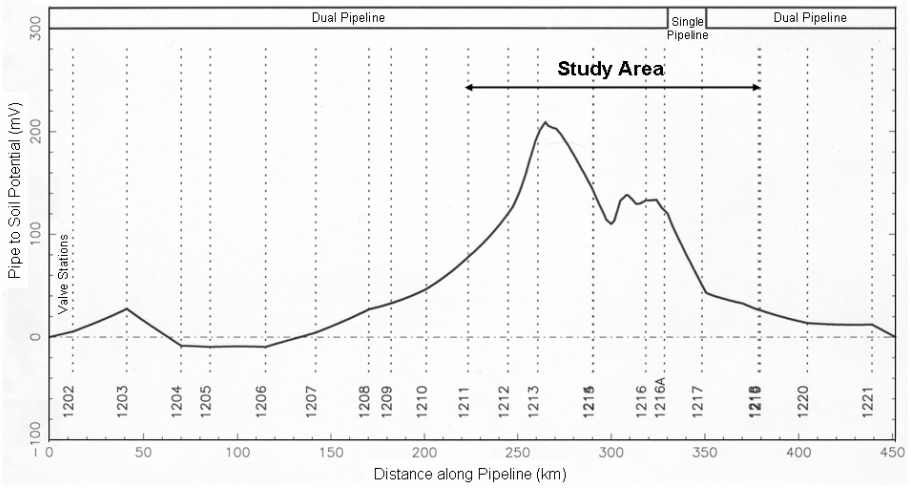

Fig. 8. Modelled PSP for the entire 450 km long branch of pipeline from North Bay (km 0) to Morrisburg (km 450).

perpendicular to the pipe $H_{\perp}$ can be used to calculate the geoelectric field parallel to the pipeline.

Assuming a magnetic field variation of 1 nanotesla (nT), the geoelectric field $\boldsymbol{E}$ is numerically the same as the Z_{yx} (45) impedance value obtained from the MT soundings, as follows:

$$E\left(\frac{\mathrm{mV}}{\mathrm{km}}\right) = Z_{yx}(45)\left(\frac{\mathrm{mV}}{\mathrm{km}\cdot\mathrm{nT}}\right)\cdot 1\,(\mathrm{nT})\,. \tag{6}$$

Impedances at a frequency of 0.01 Hz were chosen for pipeline modelling as representative of overall crustal geology. At this frequency, the effective depth of MT imaging of the subsurface ranges from about 20 to 55 km based on an apparent resistivity range of 500–3000 Ω m (see Fig. 7a). The change of Z_{yx} (45) surface impedance across the pipeline route is shown as the dashed line in Fig. 7b.

To validate the measured Z_{yx} (45) surface impedance against impedances generated by the 2-D inversion WinGlink modelling software (which produced the resistivity cross-section seen in Fig. 7a) we extracted the modelled (and rotated) Z_{yx} impedances at eight different frequencies ranging from 0.001 to 6810 Hz. The uppermost frequency was limited by input editing and the software so as to provide the most reliable estimate of resistivity. Figure 7b shows there to be a close agreement of measured and modelled Z_{yx} impedances, except at MT Site ORF150.

Figure 7b also shows a trend for the geoelectric field, which is represented by Z_{yx} (45) impedance, to increase (for frequencies at or below 1 Hz) as the profile approaches the intensely sheared gneissic rock of the Central Metasedimentary Belt boundary thrust zone. Superimposed on this trend are peaks and troughs where the geoelectric field abruptly changes, however, some changes are only apparent at or accentuated at higher frequencies.

The greatest variation of geoelectric field (across all frequencies) is situated over the Pakenham Dome (intrusive A) where there are additional complicating geological features such as the Pakenham Fault, contact with the Paleozoic cover rock and overlying conductive Leda clays. Geoelectric field variation over the Hurds Lake pluton (intrusive B), where faults and tectonic terrane boundaries also occur, are only noticeable at the two highest frequencies. As the Bonnechere Ridge (intrusive C) is approached, the geoelectric field amplitude increases with increasing frequency. A small but persistent change across all geoelectric field frequencies occurs in the vicinity of MT sites ORV2 to ORF130. Here, underlying the Paleozoic rock, is a resistive orbicular body similar to the other intrusives. In addition, the geoelectric field change roughly coincides with the boundary between the Frontenac and Sharbot Lake tectonic terranes.

4 Pipeline modelling

The effect of electric fields induced in pipelines can be modelled using the distributed-source transmission line (DSTL) theory first described in Schelkunoff (1943). DSTL theory was adapted by Boteler and Cookson (1986) for the study of geomagnetic induction in pipelines and has since been used in a number of studies (Edwall and Boteler, 2001; Pulkkinen et al., 2001b; Rix and Boteler, 2001; Trichtchenko et al., 2001). The theory incorporates the combined effects from electrical properties of the pipe itself, the Earth conductivity structure, and the induced electric field generated by geomagnetic variations.

In the DSTL approach, the pipeline is represented as a transmission line, modeled by invoking multiple segments of different lengths and orientations to represent the path of the pipeline along its route (Boteler, 1997). The induced electric field is represented by voltage sources distributed along the transmission line. The electrical properties of the pipeline are the series impedance per unit length,

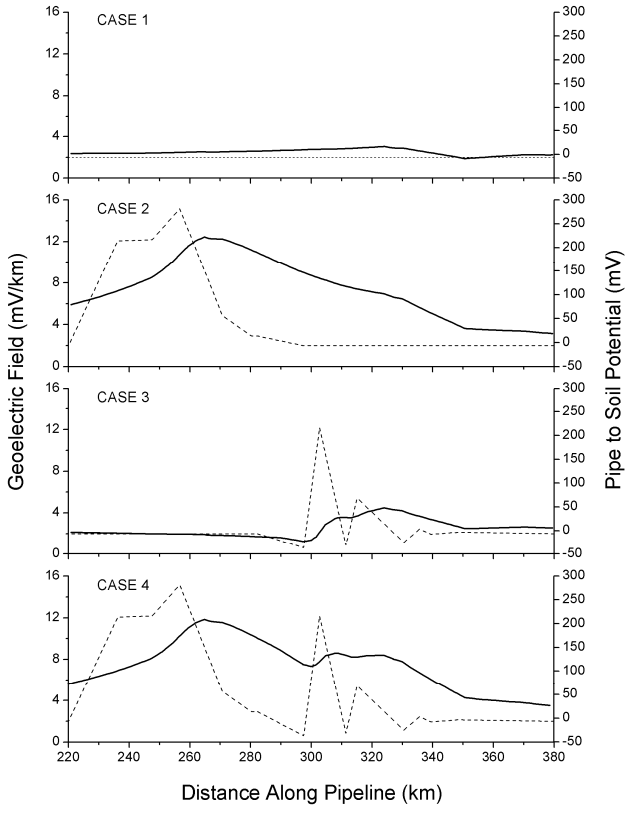

Fig. 9. Modelled PSP variations and calculated non-uniform geoelectric field versus distance along pipeline, as derived from all measured Z_{yx} (45) impedances between: km 235 and km 350 for Case 1; km 245 and km 270 for Case 2; 290 and km 340 for Case 3; and, km 235 and km 350 for Case 4. Solid line represents the pipe-to-soil potential. Dashed line represents the geoelectric field (0.01 Hz) – assuming a 1 nT variation of the geomagnetic field – along general alignment of pipeline.

Z_{pipe}, given by the resistivity of the pipeline steel and cross-sectional area of the pipe, and the parallel admittance per unit length, Y_{pipe}, given by the conductance through the pipeline coating. These parameters determine the propagation constant, $\gamma = \sqrt{Z\text{pipe} \cdot Y\text{pipe}}$ and the characteristic impedance, $Zo = \sqrt{Z\text{pipe}/Y\text{pipe}}$.

Along most of the route there are two pipelines in parallel. For individual pipelines with series impedance Z_{pipe} and parallel admittance Y_{pipe}, the effective series impedance of the two parallel pipelines is $Z\text{pipe}/2$ and their effective parallel admittance is $2Y_{\text{pipe}}$. This causes a reduction in the characteristic impedance which is now $Zo = \frac{1}{2}\sqrt{Z\text{pipe}/Y\text{pipe}}$. However, the propagation constant is unchanged at $\gamma = \sqrt{Z\text{pipe} \cdot Y\text{pipe}}$ as the differences in Z_{pipe} and Y_{pipe} cancel (Boteler, 2000).

For this study a DSTL model was set up for the 450 km pipeline from North Bay to Morrisburg. The pipeline consisted of dual line throughout the length of the route, except for a 20 km long single pipe segment between valve stations 1216A and 1217 (km 328 and km 348) (Fig. 8). The single pipe segment is electrically connected to the double pipelines at either end so the only discontinuity is caused by the change in series impedance and parallel admittance described above. At the ends of the pipeline a terminating resistance of 0.1 Ω m was used to represent the connection to the rest of the pipeline network. The other inputs to the pipeline model are pipe electrical properties (Table 2) – provided by the pipeline operator for the international telluric study in 1997 (Boteler and Trichtchenko, 2000) – and the geoelectric field derived from the measured MT impedances. Figure 8 shows the modelled pipeline response to this geoelectric field and clearly shows the large PSP variations in the study area.

Table 2. Electrical properties of the pipeline of interest between North Bay and Morrisburg (from Boteler and Trichtchenko, 2000).

		Single pipe	Double pipe
Coating conductance	(μS m^{-2})	20	20
Series resistance	(Ω km^{-1})	0.008	0.004
Parallel admittance	(S km^{-1})	0.056	0.112
Characteristic impedance	(Ω)	0.378	0.189
Propagation constant	(km^{-1})	0.021	0.021
Adjustment distance	(km)	47	47

4.1 Modelling results

To examine the effect of the geoelectric field changes identified by the MT study we focus on the DSTL modelling results for the portion of the pipeline within the study area, between valve stations 1211 and 1218 (km 223 to km 378).

Based on rotated Z_{yx} (45) impedances and a magnetic field variation of 1 nT at a frequency of 0.01 Hz, the calculated geoelectric field along the pipeline route is comprised of a base level of 2 mV/km at the southeast end, stepping up to about 13 mV/km in the northwest near km 260, with additional peaks, ranging from 12 to 2.5 mV/km, between km 290 and km 330.

The following four (Fig. 9) cases of the geoelectric field were constructed and the corresponding PSPs were computed.

In Case 1, a uniform geoelectric field of 2 mV/km is assumed. This is based on the surface impedance at the east end of the pipeline (see Fig. 7b). The Case 1 model was done to show the effects of pipeline structure alone on PSP amplitudes, independent of changes in the geoelectric field. The PSP is small over most of the pipeline reaching peak values of +15 mV and −10 mV associated with an

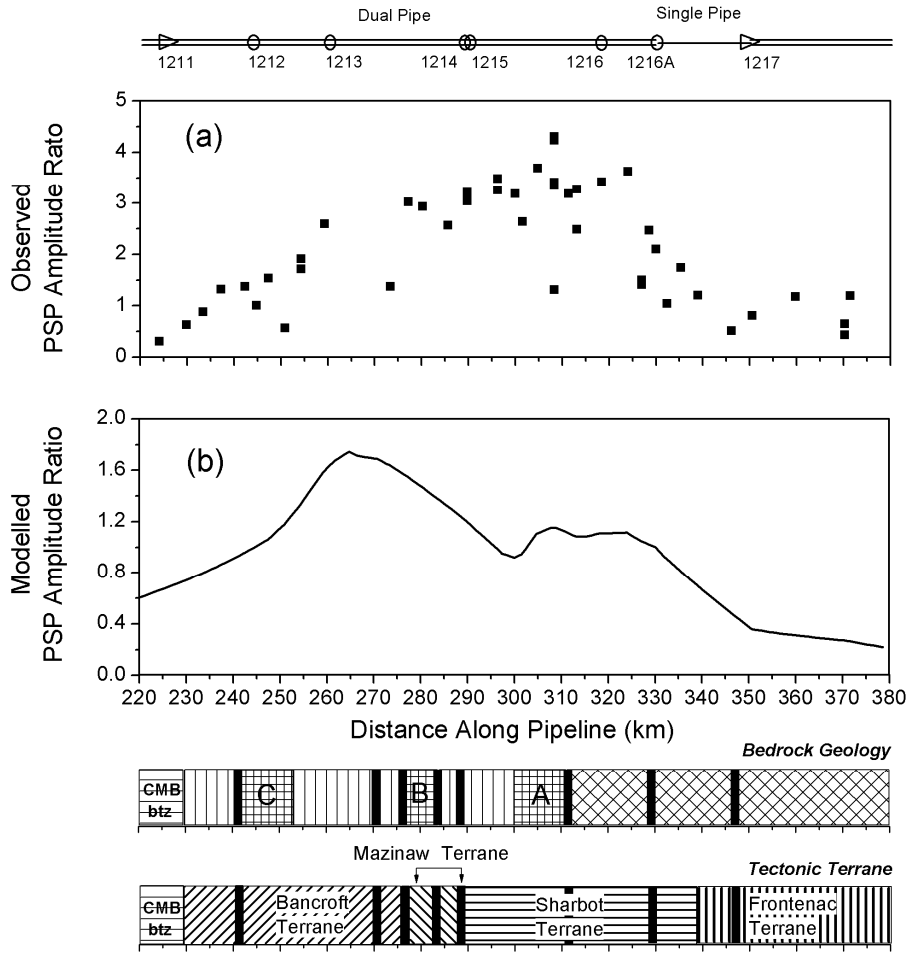

Fig. 10. Comparison of observed PSP amplitude ratio **(a)** and the Case 4 modelled PSP amplitude ratio **(b)** variations along the pipeline. Schematic representation of pipeline structure shown at top of figure (see Fig. 5 for key). Schematic representation of bedrock geology (see Fig. 7 for key) and tectonic terrane along the pipeline route are shown at bottom of figure.

increased potential gradient over the single pipe section between km 328 and km 348.

In Case 2, the step-up in the calculated geoelectric field at the northwest portion is examined. For positions west of km 290, a spatially varying geoelectric field derived from the impedance in Fig. 7b is used. A uniform geoelectric field of 2 mV/km is used east of km 290. The modelled PSP amplitude shows a broad elevated response between km 220 and 351, peaking in the vicinity of MT site ORV5 (km 257). Compared to Case 1, the PSP amplitude is much larger than the contribution from the pipe structure itself.

In Case 3, the effect of two peaks of the geoelectric field, between km 290 and km 340, are examined. For positions east of km 290, a spatially varying geoelectric field derived from the impedance in Fig. 7b is used. A uniform geoelectric field of 2 mV/km is used west of km 290. There is a moderate enhancement of the modelled PSP amplitude between km 305 and km 351.

In Case 4, the complete spatial variation of the calculated geoelectric field along the pipeline, including both the step-up in the northwest portion and the two peaks in the southeast portion, is incorporated. The enhancement of the modelled PSP amplitude occurs in the same areas as for Cases 2 and 3. The PSP amplitude between km 305 and km 351, however, is broader than for Case 3.

Comparing the Case 4 modelled PSP (rescaled as an amplitude ratio) with observed PSP amplitude ratios (Fig. 10) shows that both indicate a broad peak in PSP amplitudes within the study area. Variations in the modelled and observed PSP amplitude occur in approximately the same areas along the pipeline, as well as having a similar trend compared to each other. Specifically, there is an increase of PSP amplitude between km 250 and km 335. In the southeast portion of the study area, the broad peak in PSP amplitude between km 305 and km 328 can be considered to be reasonably valid on the basis of the higher density of PSP recordings and

closer spacing of MT sites. In the northwest portion of the study area, the PSP amplitude peak in the vicinity of MT site ORV5 (near km 257) is not as well defined because of a lesser density of PSP recordings and MT sites.

5 Conclusions

To test the hypothesis that the large PSP variations observed along the pipeline of interest in the study area are related to the local geology, we established a link between the electrical properties of geological features and PSP amplitudes via the calculation of surface impedances based on MT data. Both observed and modelled PSP amplitudes confirm that a zone of enhanced PSP variation occurs in the same area (between MT sites ORF140 and ORF150) as previously identified in the 1997 study by Boteler and Trichtchenko (2000).

A MT resistivity cross-section revealed the presence of several electrically resistive, intrusive bodies, in the first 6 to 12 km of the crust, some of which coincide with impedance peaks at a number of frequencies. Our modelled PSP amplitudes – using a constant surface geoelectric field – have shown that changes in pipeline structure have only a small effect on resultant PSP amplitudes. Such changes are not sufficient to account for the enhanced amplitudes seen in the observed PSP data. Only when geoelectric field peaks are taken into account in pipeline modelling did the ratio of observed PSPs and modelled PSPs provide a better match. The match was particularly convincing for the impedance peaks at MT sites ORF145, ORF140 and ORF120/ORV2 where the resistivity cross-section indicates the presence of electrically resistive zones that coincide with near-surface intrusive bodies. At these locations, the impedance peak was apparent across all frequencies sounded. It should also be noted that other geological features are present, such as faults and tectonic terrane boundaries which could be additional factors causing enough resistivity contrast to create the geoelectric field peaks and hence the large PSP amplitudes seen here. In contrast, the Hurds Lake intrusive situated beneath MT sites ORV4 and ORF160 shows only an impedance peak at the uppermost frequencies sounded. It could be due to a combination of effects including the relative size of the body, the conductivity contrast between the body and surrounding material, and local noise. More PSP and MT data are needed to confirm the peak in the modelled response in the vicinity of MT site ORV5 which was located on the flank of an intrusive. Finer spacing of the MT sites would provide better resolution in areas of rapid changes of Earth conductivity and hence, contribute in improving the fit between modelled and observed data in such areas.

The results obtained in this study indicate that ground conductivity structure has a significant effect on the size of PSP variations produced by geomagnetic induction. Further work is needed to resolve the relative size of the contribution from the Precambrian Shield/Paleozoic sedimentary boundary around km 290, the presence of resistive intrusive bodies and/or faults between km 245 and km 325 along the pipeline route, and the gross resistivity differences between the various tectonic terranes that underlie the pipeline route.

Acknowledgements. The authors want to express their thanks to G. Graham (Phoenix Geophysics Ltd.) and G. McNeice (Geosystem Canada Inc.) for guidance with MT field survey procedures and data processing. Field assistance was provided by S. Blinova, M. Folta and T. Pacha from Carleton University, and C. Andrews, M. Pearson, D. Regimbald, and A. Trichtchenko from the Ottawa Geomagnetic Laboratory. Data extraction programs were developed by D. Danskin at the laboratory. An initial review of the material presented in this paper was undertaken by I. Ferguson of the University of Manitoba. We gratefully appreciate the financial support of the pipeline company and its permission to install the data loggers, logistical support from the Geomagnetic Laboratory, and property access by landowners to allow placement of MT instruments. This manuscript benefited from the constructive reviews by the anonymous referees.

Topical Editor I. A. Daglis thanks two referees for their help in evaluating this paper.

References

Belanger, J. R.: Urban geology of Canada's National Capital area, in: Urban Geology of Canadian Cities, edited by: Karrow, P. and White, O., Geological Association of Canada Special Paper, 42, 365–384, 1998.

Beamish, D., Clark, T. D. G., Clarke, E., and Thomson, A. W. P.: Geomagnetically induced currents in the UK: geomagnetic variations and surface electric fields, J. Atmos. Solar Terr., 64, 1779–1792, 2002.

Bianchetti, R. L.: Survey method and evaluation techniques, in: Peabody's Control of Pipeline Corrosion, Second Edition, edited by: Bianchetti, R. L., NACE International, Houston, 65–100, 2001.

Boteler, D. H.: Distributed source transmission line theory for active terminations, Proc. 1997 Zurich EMC Symposium, 18–20 February, URSI supplement, 401–408, 1997.

Boteler, D. H.: Geomagnetic effects on the pipe-to-soil potentials of a continental pipeline, Adv. Space Res., 26, 15–20, 2000.

Boteler, D. H. and Cookson, M. J.: Telluric currents and their effects on pipelines in the Cook Strait region of New Zealand, Materials Performance, 25, 27–32, 1986.

Boteler, D. H., Pirjola, R. J., and Nevanlinna, H.: The effects of geomagnetic disturbances on electrical systems at the earth's surface, Adv. Space Res., 22, 17–27, 1998.

Boteler, D. H. and Trichtchenko, L.: International study of telluric current effects on pipelines, Final Report, Geological Survey of Canada, Open File 3050, 2000.

Boteler, D. H., Trichtchenko, L., and Samson, C.: Investigation of earth conductivity influence on pipe-to-soil potentials, Proceedings, NACE North Area 2003 Eastern Conference, Ottawa, Sept., 2003.

Campbell, W. H.: Induction of auroral zone electric currents within the Alaska pipeline, Pure Appl. Geophys., 116, 1143–1173, 1978.

Campbell, W. H.: Observation of electric currents in the Alaska oil pipeline resulting from auroral electrojet current sources, Geophys. J. Roy. Astr. Soc., 61, 437–449, 1980.

Carr, S. D., Easton, R. M., Jamieson, R. A., and Culshaw, N. G.: Geologic transect across the Grenville Orogen of Ontario and New York, Can. J. Earth Sci., 37, 193–216, 2000.

Edwall, H.-E. and Boteler, D. H.: Studies of Telluric Currents on Pipelines in Southern Sweden, Paper 01315, Proceedings, CORROSION 2001, NACE International, Houston, 11–16 March 2001.

Frederiksen, A. W., Ferguson, I. J., Easton, D., Miong, S.-K., and Gowan, E.: Mantle fabric at multiple scales across an Archean-Proterozoic Boundary, Eastern Ontario, Canada, Phys. Earth Planet. Inter., 158, 240–263, 2005.

Gamble, T. D., Goubau, W. M., and Clarke, J.: Magnetotellurics with a remote magnetic reference, Geophysics, 44, 53–68, 1979.

Gummow, R. A., Boteler, D. H., and Trichtchenko, L.: Telluric and ocean current effects on buried pipelines and their cathodic protection systems, Pipeline Research Council International, Inc., Contract No. PR-262-0030, 2001.

Gummow, R. A.: GIC effects on pipeline corrosion and corrosion control systems, J. Atmos. Solar Terr., 64, 1755–1764, 2002.

Hejda, P. and Bochníček, J.: Geomagnetically induced pipe-to-soil voltages in the Czech oil pipelines during October–November 2003, Ann. Geophys., 23, 3089–3093, 2005, http://www.ann-geophys.net/23/3089/2005/.

Jones, A. G. and Garcia, X.: Electrical resistivity structure of the Yellowknife River Fault zone and surrounding region, Chapter 10, in: Gold in the Yellowknife Greenstone Belt, Northwest Territories, edited by: Anglin, C. D., Falck, H., Wright, D. F., and Ambrose, E. J., Geological Association of Canada, Special Publication No. 3, 126–141, 2006.

Kaufman, A. and Keller, G.: The magnetotelluric sounding method, Elsevier Scientific Publishing Company, 1981.

Kay, S.: Fundamentals of statistical signal processing, vol. 1 Estimation theory, Prentice-Hall, Englewood Cliffs, New Jersey, 1993.

Lanzerotti, L. J. and Gregori, G. P.: Telluric currents: The natural environment and interactions with man-made systems, in: The Earth's electrical environment, National Academy Press, 232–257, 1986.

Osella, A. and Favetto, A.: Effects of soil resistivity on currents induced on pipelines, J. Appl. Geophys., 44, 303–312, 2000.

Ontario Geological Survey: Bedrock geology of Ontario seamless coverage, ERLIS Data Set 6 (Digital Map File), 1993.

McKay, A. J. and Whaler, K. A.: The electric field in northern England and southern Scotland: implications for geomagnetically induced currents, Geophys. J. Int., 167, 613–625, 2006.

Percival, J. A., Bleeker, W., Cook, F. A., Rivers, T., Ross, G., and van Staal, C. R.: Panlithoprobe workshop IV: Intra-orogen correlations and comparative orogenic correlations and comparative orogenic anatomy, Geoscience Canada, 31, 23–39, 2004.

Pirjola, R.: Review of the calculation of subsurface electric and magnetic fields and of geomagnetically induced currents in ground-based technological systems, Surveys in Geophysics, 23, 71–90, 2002.

Pulkkinen, A., Viljanen, A., Pajunpää, K., and Pirjola, R. J.: Recordings and occurrence of geomagnetically induced currents in the Finnish natural gas pipeline network, J. Appl. Geophys., 48, 219–231, 2001a.

Pulkkinen, A., Pirjola, R., Boteler, D., Viljanen, A., and Yegorov, I.: Modelling of space weather effects on pipelines, J. Appl. Geophys., 48, 233–256, 2001b.

Rix, B. C. and Boteler, D. H.: Telluric current considerations in the CP design for the Maritimes and Northeast Pipeline, Paper 01317, Proceedings, CORROSION 2001, NACE International, Houston, 11–16 March 2001.

Sanford, B. V.: St. Lawrence Platform introduction, in: Sedimentary cover of the craton in Canada, edited by: Stott, D. F. and Aitken, J. D., Geological Survey of Canada, Geology of Canada No. 5, 709–722, 1993.

Schelkunoff, S.A.: Electromagnetic waves, Van Norstand, New York, 1943.

Simpson, F. and Bahr, K.: Practical magnetotellurics, Cambridge University Press, New York, 2005.

Telford, W. M., Geldart, L. P., Sheriff, R. E., and Keys, D. A.: Applied geophysics, Cambridge University Press, 1976.

Trichtchenko, L., Boteler, D. H., Hesjevik, S. M., and Birketveit, O.: The Production of Telluric Current Effects in Norway, Paper 01314, Proceedings, CORROSION 2001, NACE International, Houston, 11–16 March 2001.

Trichtchenko, L. and Boteler, D. H.: Modelling of geomagnetic induction in pipelines, Ann. Geophys., 20, 1063–1072, 2002, http://www.ann-geophys.net/20/1063/2002/.

Trichtchenko, L., Boteler, D. H., and Larocca, P.: Modeling the effect of the electromagnetic environment on pipelines, Geological Survey of Canada, Open File 4826, 2004.